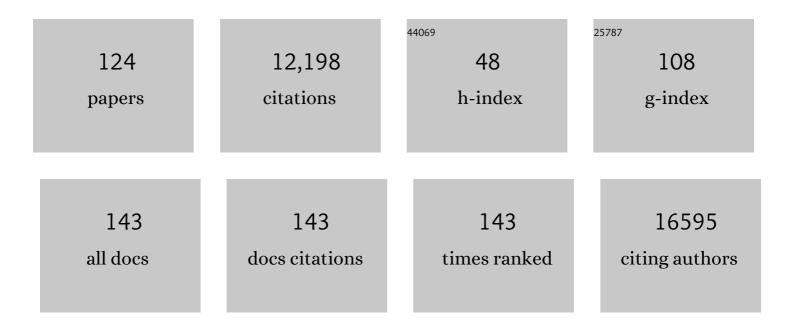
Paul Verkade

List of Publications by Year in descending order

Source: https://exaly.com/author-pdf/3591226/publications.pdf Version: 2024-02-01



#	Article	IF	CITATIONS
1	Loss of Caveolae, Vascular Dysfunction, and Pulmonary Defects in Caveolin-1 Gene-Disrupted Mice. Science, 2001, 293, 2449-2452.	12.6	1,414
2	Alzheimer's disease β-amyloid peptides are released in association with exosomes. Proceedings of the National Academy of Sciences of the United States of America, 2006, 103, 11172-11177.	7.1	1,133
3	Lipid Domain Structure of the Plasma Membrane Revealed by Patching of Membrane Components. Journal of Cell Biology, 1998, 141, 929-942.	5.2	1,118
4	Self-Assembling Cages from Coiled-Coil Peptide Modules. Science, 2013, 340, 595-599.	12.6	451
5	Tight junctions are membrane microdomains. Journal of Cell Science, 2000, 113, 1771-1781.	2.0	391
6	Nanoparticles can cause DNA damage across a cellular barrier. Nature Nanotechnology, 2009, 4, 876-883.	31.5	351
7	ESCRT-III controls nuclear envelope reformation. Nature, 2015, 522, 236-239.	27.8	305
8	Clostridium difficile Toxins Disrupt Epithelial Barrier Function by Altering Membrane Microdomain Localization of Tight Junction Proteins. Infection and Immunity, 2001, 69, 1329-1336.	2.2	300
9	Caveolin-1 and -2 in the Exocytic Pathway of MDCK Cells. Journal of Cell Biology, 1998, 140, 795-806.	5.2	283
10	Lipids as Modulators of Proteolytic Activity of BACE. Journal of Biological Chemistry, 2005, 280, 36815-36823.	3.4	260
11	The Retromer Coat Complex Coordinates Endosomal Sorting and Dynein-Mediated Transport, with Carrier Recognition by the trans-Golgi Network. Developmental Cell, 2009, 17, 110-122.	7.0	252
12	The Mammalian Staufen Protein Localizes to the Somatodendritic Domain of Cultured Hippocampal Neurons: Implications for Its Involvement in mRNA Transport. Journal of Neuroscience, 1999, 19, 288-297.	3.6	239
13	Antibacterial effects of nanopillar surfaces are mediated by cell impedance, penetration and induction of oxidative stress. Nature Communications, 2020, 11, 1626.	12.8	235
14	Raft association of SNAP receptors acting in apical trafficking in Madin-Darby canine kidney cells. Proceedings of the National Academy of Sciences of the United States of America, 1999, 96, 3734-3738.	7.1	231
15	FAPP2, cilium formation, and compartmentalization of the apical membrane in polarized Madin–Darby canine kidney (MDCK) cells. Proceedings of the National Academy of Sciences of the United States of America, 2006, 103, 18556-18561.	7.1	188
16	Constitutive activation of Rho proteins by CNF-1 influences tight junction structure and epithelial barrier function. Journal of Cell Science, 2003, 116, 725-742.	2.0	184
17	Annexin XIIIb Associates with Lipid Microdomains to Function in Apical Delivery. Journal of Cell Biology, 1998, 142, 1413-1427.	5.2	172
18	Phase coexistence and connectivity in the apical membrane of polarized epithelial cells. Proceedings of the National Academy of Sciences of the United States of America, 2006, 103, 329-334.	7.1	160

#	Article	lF	CITATIONS
19	Efficient coupling of Sec23-Sec24 to Sec13-Sec31 drives COPII-dependent collagen secretion and is essential for normal craniofacial development. Journal of Cell Science, 2008, 121, 3025-3034.	2.0	158
20	Polypyrimidine tract-binding protein promotes insulin secretory granule biogenesis. Nature Cell Biology, 2004, 6, 207-214.	10.3	155
21	Tight junctions are membrane microdomains. Journal of Cell Science, 2000, 113 (Pt 10), 1771-81.	2.0	155
22	Moving EM: the Rapid Transfer System as a new tool for correlative light and electron microscopy and high throughput for highâ€pressure freezing. Journal of Microscopy, 2008, 230, 317-328.	1.8	152
23	SNX–BAR proteins in phosphoinositide-mediated, tubular-based endosomal sorting. Seminars in Cell and Developmental Biology, 2010, 21, 371-380.	5.0	150
24	SNX–BARâ€Mediated Endosome Tubulation is Coâ€ordinated with Endosome Maturation. Traffic, 2012, 13, 94-107.	2.7	143
25	Organisation of human ER-exit sites: requirements for the localisation of Sec16 to transitional ER. Journal of Cell Science, 2009, 122, 2924-2934.	2.0	139
26	PKCα regulates platelet granule secretion and thrombus formation in mice. Journal of Clinical Investigation, 2009, 119, 399-407.	8.2	136
27	Apical Membrane Targeting of Nedd4 Is Mediated by an Association of Its C2 Domain with Annexin Xiiib. Journal of Cell Biology, 2000, 149, 1473-1484.	5.2	135
28	Engineered synthetic scaffolds for organizing proteins within the bacterial cytoplasm. Nature Chemical Biology, 2018, 14, 142-147.	8.0	128
29	Caveolin-1 is required for fatty acid translocase (FAT/CD36) localization and function at the plasma membrane of mouse embryonic fibroblasts. Biochimica Et Biophysica Acta - Molecular and Cell Biology of Lipids, 2006, 1761, 416-423.	2.4	124
30	p75NTR-dependent activation of NF-κB regulates microRNA-503 transcription and pericyte–endothelial crosstalk in diabetes after limb ischaemia. Nature Communications, 2015, 6, 8024.	12.8	119
31	Recent Advances in High-Pressure Freezing. Methods in Molecular Biology, 2007, 369, 143-173.	0.9	118
32	Mucosal Reactive Oxygen Species Decrease Virulence by Disrupting Campylobacter jejuni Phosphotyrosine Signaling. Cell Host and Microbe, 2012, 12, 47-59.	11.0	118
33	Infectious Bronchitis Virus Generates Spherules from Zippered Endoplasmic Reticulum Membranes. MBio, 2013, 4, e00801-13.	4.1	118
34	Induction of Caveolae in the Apical Plasma Membrane of Madin-Darby Canine Kidney Cells. Journal of Cell Biology, 2000, 148, 727-740.	5.2	105
35	The 2018 correlative microscopy techniques roadmap. Journal Physics D: Applied Physics, 2018, 51, 443001.	2.8	99
36	FAPP2 is involved in the transport of apical cargo in polarized MDCK cells. Journal of Cell Biology, 2005, 170, 521-526.	5.2	95

#	Article	IF	CITATIONS
37	Long-Chain Fatty Acid Uptake into Adipocytes Depends on Lipid Raft Function. Biochemistry, 2004, 43, 4179-4187.	2.5	93
38	Lipid microdomains and membrane trafficking in mammalian cells. Histochemistry and Cell Biology, 1997, 108, 211-220.	1.7	71
39	Cryo-transmission electron microscopy structure of a gigadalton peptide fiber of de novo design. Proceedings of the National Academy of Sciences of the United States of America, 2012, 109, 13266-13271.	7.1	70
40	Studying intracellular transport using high-pressure freezing and Correlative Light Electron Microscopy. Seminars in Cell and Developmental Biology, 2009, 20, 910-919.	5.0	68
41	A role for Rab14 in the endocytic trafficking of GLUT4 in 3T3-L1 adipocytes. Journal of Cell Science, 2013, 126, 1931-41.	2.0	67
42	Lactose as a "Trojan Horse―for Quantum Dot Cell Transport. Angewandte Chemie - International Edition, 2014, 53, 810-814.	13.8	67
43	Mother Centriole Distal Appendages Mediate Centrosome Docking at the Immunological Synapse and Reveal Mechanistic Parallels with Ciliogenesis. Current Biology, 2015, 25, 3239-3244.	3.9	63
44	REMBI: Recommended Metadata for Biological Images—enabling reuse of microscopy data in biology. Nature Methods, 2021, 18, 1418-1422.	19.0	63
45	Involvement of caveolin-2 in caveolar biogenesis in MDCK cells. FEBS Letters, 2003, 538, 85-88.	2.8	62
46	Correlated Multimodal Imaging in Life Sciences: Expanding the Biomedical Horizon. Frontiers in Physics, 2020, 8, .	2.1	61
47	Novel standards in the measurement of rat insulin granules combining electron microscopy, high-content image analysis and in silico modelling. Diabetologia, 2012, 55, 1013-1023.	6.3	59
48	The use of markers for correlative light electron microscopy. Protoplasma, 2010, 244, 91-97.	2.1	55
49	Decorating Self-Assembled Peptide Cages with Proteins. ACS Nano, 2017, 11, 7901-7914.	14.6	55
50	Preface. Methods in Cell Biology, 2012, 111, xvii-xix.	1.1	48
51	A 3D cellular context for the macromolecular world. Nature Structural and Molecular Biology, 2014, 21, 841-845.	8.2	47
52	Intracellular Membrane Traffic at High Resolution. Methods in Cell Biology, 2010, 96, 619-648.	1.1	46
53	Volume electron microscopy. Nature Reviews Methods Primers, 2022, 2, .	21.2	46
54	Molecular Mechanism of Myosin Va Recruitment to Dense Core Secretory Granules. Traffic, 2012, 13, 54-69.	2.7	45

#	Article	IF	CITATIONS
55	Different properties of two isoforms of annexin XIII in MDCK cells. Journal of Cell Science, 2000, 113, 2607-2618.	2.0	44
56	Caveolin-1 Is Not Essential for Biosynthetic Apical Membrane Transport. Molecular and Cellular Biology, 2005, 25, 10087-10096.	2.3	43
57	Mice Lacking the Nuclear Pore Complex Protein ALADIN Show Female Infertility but Fail To Develop a Phenotype Resembling Human Triple A Syndrome. Molecular and Cellular Biology, 2006, 26, 1879-1887.	2.3	41
58	MiR-3120 Is a Mirror MicroRNA That Targets Heat Shock Cognate Protein 70 and Auxilin Messenger RNAs and Regulates Clathrin Vesicle Uncoating. Journal of Biological Chemistry, 2012, 287, 14726-14733.	3.4	41
59	High-Contrast Imaging of Nanodiamonds in Cells by Energy Filtered and Correlative Light-Electron Microscopy: Toward a Quantitative Nanoparticle-Cell Analysis. Nano Letters, 2019, 19, 2178-2185.	9.1	40
60	De novo targeting to the cytoplasmic and luminal side of bacterial microcompartments. Nature Communications, 2018, 9, 3413.	12.8	39
61	Cellular uptake and targeting of low dispersity, dual emissive, segmented block copolymer nanofibers. Chemical Science, 2020, 11, 8394-8408.	7.4	39
62	B-50/GAP-43 Potentiates Cytoskeletal Reorganization in Raft Domains. Molecular and Cellular Neurosciences, 1999, 14, 85-97.	2.2	34
63	Islet Cell Autoantigen of 69 kDa Is an Arfaptin-related Protein Associated with the Golgi Complex of Insulinoma INS-1 Cells. Journal of Biological Chemistry, 2003, 278, 26166-26173.	3.4	33
64	In vitro placenta barrier model using primary human trophoblasts, underlying connective tissue and vascular endothelium. Biomaterials, 2019, 192, 140-148.	11.4	33
65	In situ cryo-electron tomography reveals filamentous actin within the microtubule lumen. Journal of Cell Biology, 2020, 219, .	5.2	32
66	Prior exercise in humans redistributes intramuscular GLUT4 and enhances insulin-stimulated sarcolemmal and endosomal GLUT4 translocation. Molecular Metabolism, 2020, 39, 100998.	6.5	29
67	The actinâ€driven spatiotemporal organization of Tâ€cell signaling at the system scale. Immunological Reviews, 2013, 256, 133-147.	6.0	27
68	Ultrastructural co-localization of calmodulin and B-50/growth-associated protein-43 at the plasma membrane of proximal unmyelinated axon shafts studied in the model of the regenerating rat sciatic nerve. Neuroscience, 1997, 79, 1207-1218.	2.3	26
69	Modifying Self-Assembled Peptide Cages To Control Internalization into Mammalian Cells. Nano Letters, 2018, 18, 5933-5937.	9.1	26
70	Computational spatiotemporal analysis identifies WAVE2 and cofilin as joint regulators of costimulation-mediated T cell actin dynamics. Science Signaling, 2016, 9, rs3.	3.6	24
71	SNX15 links clathrin endocytosis to the PtdIns(3)P early endosome independent of the APPL1 endosome. Journal of Cell Science, 2013, 126, 4885-99.	2.0	22
72	Capturing Endocytic Segregation Events with HPF-CLEM. Methods in Cell Biology, 2012, 111, 175-201.	1,1	21

#	Article	IF	CITATIONS
73	Preface. Methods in Cell Biology, 2014, 124, xvii-xviii.	1.1	21
74	Infectious Bronchitis Virus Nonstructural Protein 4 Alone Induces Membrane Pairing. Viruses, 2018, 10, 477.	3.3	20
75	Correlative two-photon and serial block face scanning electron microscopy in neuronal tissue using 3D near-infrared branding maps. Methods in Cell Biology, 2017, 140, 245-276.	1.1	19
76	Species differences in the morphology of transverse tubule openings in cardiomyocytes. Europace, 2018, 20, iii120-iii124.	1.7	19
77	Nano-scale morphology of cardiomyocyte t-tubule/sarcoplasmic reticulum junctions revealed by ultra-rapid high-pressure freezing and electron tomography. Journal of Molecular and Cellular Cardiology, 2021, 153, 86-92.	1.9	19
78	Molecular Etiology of Atherogenesis – In Vitro Induction of Lipidosis in Macrophages with a New LDL Model. PLoS ONE, 2012, 7, e34822.	2.5	19
79	Early Signaling in Primary T Cells Activated by Antigen Presenting Cells Is Associated with a Deep and Transient Lamellal Actin Network. PLoS ONE, 2015, 10, e0133299.	2.5	19
80	De Novo Designed Peptide and Protein Hairpins Selfâ€Assemble into Sheets and Nanoparticles. Small, 2021, 17, e2100472.	10.0	18
81	PKCÎ, links proximal T cell and Notch signaling through localized regulation of the actin cytoskeleton. ELife, 2017, 6, .	6.0	18
82	Maintenance of complex I and its supercomplexes by NDUF-11 is essential for mitochondrial structure, function and health. Journal of Cell Science, 2021, 134, .	2.0	17
83	The increase in B-50/GAP-43 in regenerating rat sciatic nerve occurs predominantly in unmyelinated axon shafts: A quantitative ultrastructural study. Journal of Comparative Neurology, 1995, 356, 433-443.	1.6	16
84	Development of a quantitative Correlative Light Electron Microscopy technique to study GLUT4 trafficking. Protoplasma, 2014, 251, 403-416.	2.1	16
85	Bioinspired Silicification Reveals Structural Detail in Self-Assembled Peptide Cages. ACS Nano, 2018, 12, 1420-1432.	14.6	16
86	Different properties of two isoforms of annexin XIII in MDCK cells. Journal of Cell Science, 2000, 113 () Tj ETQq0	0 Q rgBT /	Overlock 101
87	Endothelial glycocalyx is damaged in diabetic cardiomyopathy: angiopoietin 1 restores glycocalyx and improves diastolic function in mice. Diabetologia, 2022, 65, 879-894.	6.3	15
88	Retracing in Correlative Light Electron Microscopy. Methods in Cell Biology, 2014, 124, 1-21.	1.1	14
89	Direct Evidence of Lack of Colocalisation of Fluorescently Labelled Gold Labels Used in Correlative Light Electron Microscopy. Scientific Reports, 2017, 7, 44666.	3.3	14
90	Lipid species affect morphology of endoplasmic reticulum: a sea urchin oocyte model of reversible manipulation. Journal of Lipid Research, 2019, 60, 1880-1891.	4.2	14

6

#	Article	IF	CITATIONS
91	Effect of metabolosome encapsulation peptides on enzyme activity, coaggregation, incorporation, and bacterial microcompartment formation. MicrobiologyOpen, 2020, 9, e1010.	3.0	14
92	Ultrastructural Correlates of Enhanced Norepinephrine and Neuropeptide Y Cotransmission in the Spontaneously Hypertensive Rat Brain. ASN Neuro, 2015, 7, 175909141561011.	2.7	13
93	The interaction of Escherichia coli O157 :H7 and Salmonella Typhimurium flagella with host cell membranes and cytoskeletal components. Microbiology (United Kingdom), 2020, 166, 947-965.	1.8	12
94	Ultrastructural localization of B-50/growth-associated protein-43 to anterogradely transported synaptophysin-positive and calcitonin gene-related peptide-negative vesicles in the regenerating rat sciatic nerve. Neuroscience, 1996, 71, 489-505.	2.3	11
95	Ultrastructural evidence for the lack of co-transport of B-50/GAP-43 and calmodulin in myelinated axons of the regenerating rat sciatic nerve. Journal of Neurocytology, 1996, 25, 583-595.	1.5	11
96	Optical micro-spectroscopy of single metallic nanoparticles: quantitative extinction and transient resonant four-wave mixing. Faraday Discussions, 2015, 184, 305-320.	3.2	11
97	Endocytosis in flight-stimulated adipokinetic cells ofLocusta migratoria. Cell and Tissue Research, 1993, 271, 485-489.	2.9	10
98	Modest Interference with Actin Dynamics in Primary T Cell Activation by Antigen Presenting Cells Preferentially Affects Lamellal Signaling. PLoS ONE, 2015, 10, e0133231.	2.5	8
99	A Novel Framework for Segmentation of Secretory Granules in Electron Micrographs. Medical Image Analysis, 2014, 18, 411-424.	11.6	7
100	Correlative Light and Electron Microscopy of Influenza Virus Entry and Budding. Methods in Molecular Biology, 2018, 1836, 237-260.	0.9	7
101	Transient protein accumulation at the center of the T cell antigen-presenting cell interface drives efficient IL-2 secretion. ELife, 2019, 8, .	6.0	7
102	Acute depletion of diacylglycerol from the cis-Golgi affects localized nuclear envelope morphology during mitosis. Journal of Lipid Research, 2018, 59, 1402-1413.	4.2	6
103	Correlative multimodal imaging: Building a community. Methods in Cell Biology, 2021, 162, 417-430.	1.1	6
104	Local accumulations of B-50/GAP-43 evoke excessive bleb formation in PC12 cells. Molecular Neurobiology, 1999, 20, 17-28.	4.0	5
105	Probing the future of correlative microscopy. Journal of Chemical Biology, 2015, 8, 127-128.	2.2	5
106	Using size-selected gold clusters on graphene oxide films to aid cryo-transmission electron tomography alignment. Scientific Reports, 2015, 5, 9234.	3.3	5
107	Small-residue packing motifs modulate the structure and function of a minimal de novo membrane protein. Scientific Reports, 2020, 10, 15203.	3.3	5
108	Fluorescent platinum nanoclusters as correlative light electron microscopy probes. Methods in Cell Biology, 2021, 162, 39-68.	1.1	5

#	Article	IF	CITATIONS
109	Refining a correlative light electron microscopy workflow using luminescent metal complexes. Methods in Cell Biology, 2021, 162, 69-87.	1.1	4
110	Correlative Light and Electron Microscopy with High Time Resolution and Ultrastructural Preservation. Microscopy and Microanalysis, 2005, 11, .	0.4	2
111	Quantitative biological measurement in Transmission Electron Tomography. Journal of Physics: Conference Series, 2012, 371, 012019.	0.4	2
112	Feature-based registration for correlative light and electron microscopy images. , 2014, , .		2
113	Joint denoising and contrast enhancement for light microscopy image sequences. , 2014, , .		2
114	A novel approach to identifying merging/splitting events in time-lapse microscopy. , 2016, , .		2
115	Preface to CLEM IV: Broaden the horizon. Methods in Cell Biology, 2021, 162, xix.	1.1	2
116	Active contour based segmentation for insulin granule cores in electron micrographs of beta islet cells. , 2012, 2012, 5339-42.		1
117	RJMCMC-based tracking of vesicles in fluorescence time-lapse microscopy. , 2015, , .		1
118	Insulin Granule Segmentation in 3-D TEM Beta Cell Tomograms. , 2013, , .		1
119	High-pressure Freezing in CLEM. Imaging & Microscopy, 2007, 9, 49-51.	0.1	0
120	A novel 2D and 3D method for automated insulin granule measurement and its application in assessing accepted preparation methods for electron microscopy. Journal of Physics: Conference Series, 2014, 522, 012022.	0.4	0
121	In vivo characterisation of the Golgi matrix protein giantin: linking extracellular matrix secretion and cilia function. Cilia, 2015, 4, .	1.8	0
122	Important steps in a Correlative Light Electron Microscopy Experiment. Microscopy and Microanalysis, 2015, 21, 387-388.	0.4	0
123	CLEM, 1+1 =3. Microscopy and Microanalysis, 2017, 23, 1270-1271.	0.4	0
124	High-Contrast Imaging of Nanodiamonds in Cells by Energy Filtered and Correlative Light-Electron Microscopy: Towards a Quantitative Nanoparticle-Cell Analysis. Microscopy and Microanalysis, 2019, 25, 1056-1057.	0.4	0